Center for Materials Research
Stanford University
Stanford, California

GENERATION OF COHERENT VUV AND SOFT X-RAYS.

Semiannual Report No. 2

1 January 1976 – 30 June 1976

Principal Investigators:

S. E. Harris
J. F. Young
(415) 497-0224

Sponsored by
Advanced Research Projects Agency
ARPA Order No. 2782

Contract N00014-75-C-1175 ARPA Order-2782
Program Code Number 4D10
Contract Period: 1 July 1975 – 30 September 1977
Amount of Contract: $337,500.00
Form Approved, Budget Bureau – No. 22R0293

Scientific Officer:

Director, Physics Program
Physical Sciences Division
Office of Naval Research
Department of the Navy
800 North Quincy Street
Arlington, Virginia 22217

C.M.R. Report No. 76-10

G.L. Report No. 2594

July 1976

27 p.

I. TECHNICAL SUMMARY

The goal of this program is the generation of coherent vacuum ultraviolet and soft x-ray radiation. During this reporting period our efforts have been concentrated on three frequency summing in Ne, described in Section II.

Our studies of the feasibility of using optically induced energy exchange collisions for short wavelength lasers has been suspended in order to concentrate our efforts on the harmonic generation scheme. In addition, we no longer believe that the previously reported experiment can be considered a demonstration of optically induced collisions. Details of the difficulty are given in Appendix A, the text of a paper presented at the International Conference on Tunable Lasers and Applications. Further effort at demonstrating the effect is continuing under the Office of Naval Research and the U.S. Energy Research and Development Administration sponsorship.

II. HARMONIC GENERATION OF EXTREME UV RADIATION

(K. S. Hsu, L. J. Zych, J. F. Young, and S. E. Harris)

The goal of this project is to generate coherent extreme UV (1000-300 Å) and soft x-ray (300-2 Å) radiation using a nonlinear frequency up-conversion method. As described previously, the conversion efficiency of the mixing process is enhanced by choosing two of the input frequencies so that they sum to a non-allowed atomic transition. We chose neon, because resonant two-photon-pumped sum generation in neon is simplified by a natural near coincidence of the 2p-3p non-allowed transition and the 16th harmonic of the Nd:YAG laser frequency. We are using the 7th and 9th Nd:YAG harmonics which sum to the 16th harmonic; this fact greatly simplifies the experimental apparatus. The difficulty of this approach lies in a high absorption coefficient of almost all solids at 1182 Å. In the past six months our main effort has been directed towards efficient combining of 1520 Å and 1182 Å radiation, and monitoring spatial, temporal, and frequency overlaps.

Figure 1 is an energy level diagram of our proposed experiment. Input wavelengths of 1182 Å, 1520 Å, and 10,640 Å are summed to 626 Å. The third input wavelength of 10,640 Å was chosen for several reasons: it is naturally present in the optical path following the generation of 1182 Å and 1520 Å, and by using the scheme shown in Fig. 2 the pulse timing and

3536-1

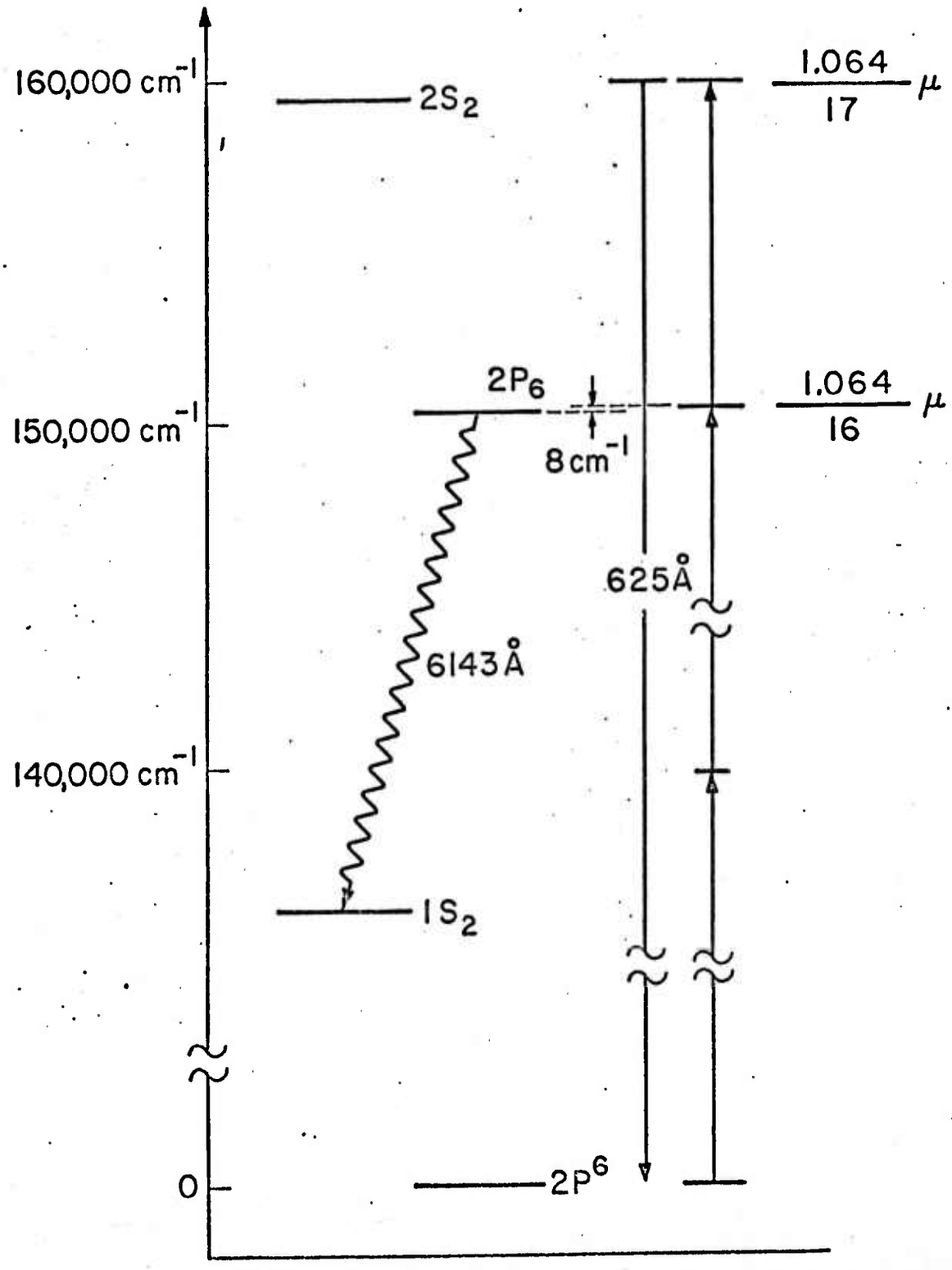

Fig. 1--Energy level diagram of neon.

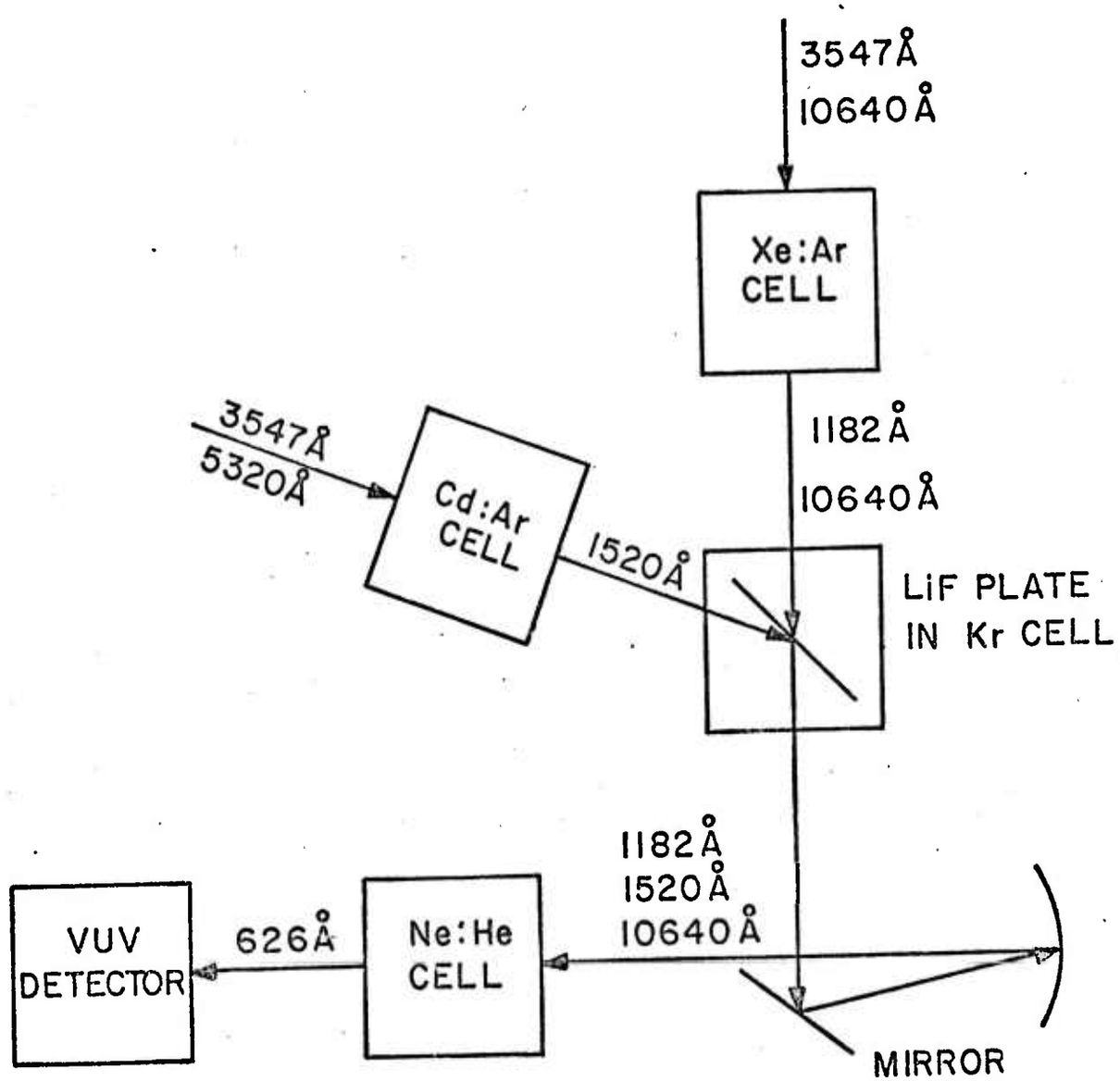

Fig. 2--Schematic of extreme UV up-conversion in neon.

power level can be adjusted easily. In addition, because the sum wavelength lies just above the Ne (4s) levels we will be able to phasematch the process as described in the last report. We have found a measurement of the neon (3s-3p) oscillator strength.[1] Using this value of 0.04, we estimate a single coherence length power conversion efficiency of 8.5×10^{-5} from 10,640 Å to 626 Å, yielding a signal-to-noise ratio greater than 100. Since 10,640 Å radiation is only 300 cm^{-1} above the neon (3s-3p) transition, the power density of 10,640 Å at the interaction zone must be limited to 5×10^{9} W/cm^2 to avoid a level shift which would destroy the resonance.

The spatial and temporal overlap of three laser beams with widely differing frequencies is a difficult technical problem. The LiF prism scheme that was proposed previously proved to be impractical, primarily because the absorption coefficient of the LiF crystal at 1182 Å was measured to be 12/inch, much larger than expected. Also, it took a very sophisticated procedure to position the 1520 Å radiation after it went through the dispersive LiF prism. A schematic of our present scheme is shown in Fig. 2. A mode-locked Nd:YAG oscillator-amplifier system, plus KDP crystals provided two separated, but synchronous 30 ps pulses of 3547 Å radiation.

A Xe:Ar cell, and a Cd:Ar cell will generate 1182 Å and 1520 Å, respectively; since both wavelengths are strongly absorbed in air the remaining beam paths are in vacuum. No suitable dielectric coatings exist; therefore, the two beams are simply combined with a 2 mm thick LiF plate. Since we do not introduce any dispersive elements we can combine the two beams by ordinary photodetector methods.

Temporal synchronization will be adjusted using two separate beam delays. A standard corner cube delay in the 1520 Å channel will be used to compensate for gross length differences between the two beam paths. The Kr cell serves as another delay device, which will delay 1182 Å in respect to 3547 Å. The separation of these two radiations is essential, since the UV (3547 Å) can ionize neon atoms from the 3p state, thus destroying the coherent excitation and nonlinear susceptibility. From the extrapolation of refractive index we estimate that one atmosphere of krypton will delay 1182 Å relative to 3547 Å by 2 - 3 picoseconds per cm.

During this period we have constructed a system to observe the Ne (3p-3s) fluorescence. As described earlier, this measurement should allow us to monitor and adjust the crystal experimental parameters without relying on the 626 Å generation process itself. The system consists of side-viewing collection optics, filters, a 1/2 meter grating monochrometer, and a sensitive photomultiplier. We have calibrated the system and verified our ability to see signals of the expected level. During the next period we will be using this system to verify our experimental variables as we attempt to generate 626 Å radiation.

References:

1. A. V. Loginov and P. F. Gruzdev, Opt. Spect. 37, 467 (1974).

III. PUBLICATIONS

1. K. S. Hsu, A. H. Kung, L. J. Zych, J. F. Young, and S. E. Harris, "1202.8 Å Generation in Hg Using a Parametrically Amplified Dye Laser," IEEE J. Quant. Elect. QE-12, 60 (January 1976).
2. D. B. Lidow, R. W. Falcone, J. F. Young, and S. E. Harris, "Inelastic Collision Induced by Intense Optical Radiation," Phys. Rev. Lett. 36, 462 (March 1976).
3. S. E. Harris, D. B. Lidow, R. W. Falcone, and J. F. Young, "Laser Induced Collisions," Proceedings of the International Conference on Tunable Lasers and Applications, Loen, Nordfjord, Norway (June 1976).

APPENDIX A

LASER INDUCED COLLISIONS

by

S. E. Harris, D. B. Lidow, R. W. Falcone, and J. F. Young

Pre-print

G. L. Report No. 2577

Contract Nos.

N00014-75-C-0576

N00014-75-C-1175

Presented at the

International Conference on

Tunable Lasers and Applications

June 7-11, 1976

at

Loen. Nordfjord, Norway

Prepared: May 1976

Edward L. Ginzton Laboratory
W. W. Hansen Laboratories of Physics
Stanford University
Stanford, California 94305

Laser Induced Collisions*

S. E. Harris, D. B. Lidow, R. W. Falcone, and J. F. Young

Edward L. Ginzton Laboratory
Stanford University, Stanford, California 94305

We describe processes where one or more photons are utilized to conserve energy between the initial and final states of colliding atoms. Energy transfer is thus initiated, and directed to particular states, by the optical radiation. A substantial difficulty with our previously reported experimental confirmation is described.

Introduction

If the energy defect of an atomic process ΔE is large with respect to kT, then the cross section for collision or chemical reaction will be quite small. In this paper we consider collision processes where one or more photons are utilized to conserve energy, i.e., $n\hbar\omega \cong \Delta E$. A prototype system is shown in Fig. 1. Energy is first stored in the designated s state of the A atom. During collision of the A and B atoms an electromagnetic field at frequency $\hbar\omega$ causes the A atom to make a virtual transition. Long range dipole-dipole coupling between the two atoms causes this excitation to be transferred to the B atom to complete the excitation. Energy transfer is thus initiated or "switched" by the presence of the optical radiation. The possibility of collision processes of this type have been predicted by GUDZENKO and YAKOVLENKO [1] and by HARRIS and LIDOW [2]. Recent theoretical work is given by PAYNE and NAYFEH [3], GELTMAN [4], and GEORGE, et al. [5]. Though an apparently successful experiment has recently been reported by LIDOW, et al. [6], as will be described subsequently, we no longer consider this experiment to be a demonstration of this effect.

NON-RESONANT INELASTIC COLLISION

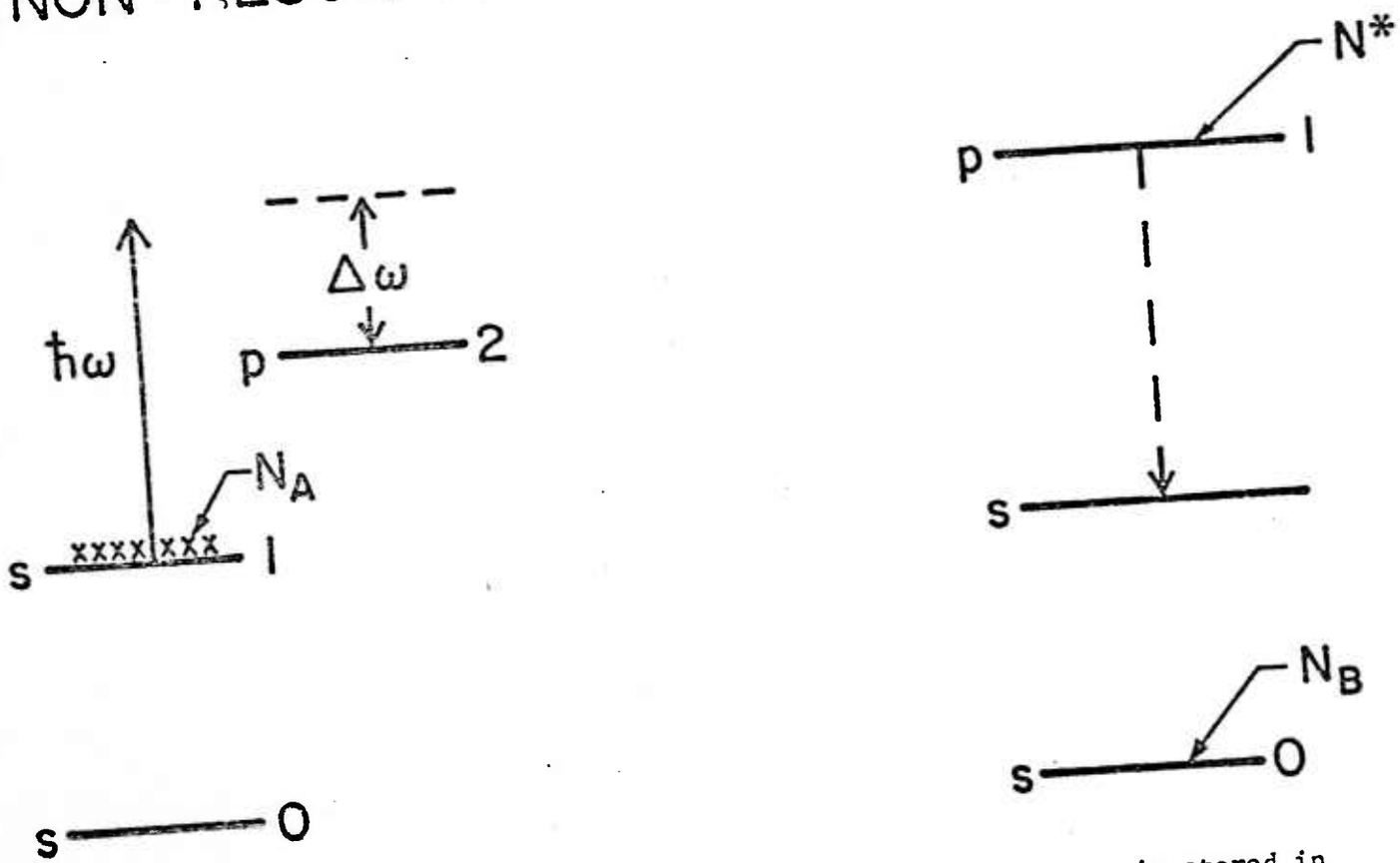

Fig. 1--Schematic of laser induced collision process. Energy is stored in the s state of atom A and may be rapidly transferred to the upper p state of atom B .

Optical processes involving the near simultaneous collision and absorption of photons may be considerably more general than that shown in Fig. 1. They may involve the absorption of several photons instead of one photon. They may take place between states involving dipole-quadrupole or quadrupole-quadrupole coupling. Processes involving charge exchange collisions, spin exchange collisions, and even free-bound reactions are possible.

Collision processes of this type may have application to the construction of short wavelength lasers, to the mapping out of interatomic potential surfaces, to the development of radiative collision and Raman lasers and frequency converters, and to the initiation of selected chemical reactions.

In the following sections of this paper I will describe these processes, summarize the theory as it is known to date, and describe a recent experimental attempt to observe a laser induced collision in a mixture of Sr and Ca.

Theory

I will first describe these effects from three related viewpoints. The first of these is the virtual transition viewpoint shown in Fig. 2. Assume first, that energy is stored in an excited s state of the first atom. In the presence of an electromagnetic field this atom makes a virtual transition. Excitation is then transferred to the second atom via dipole-dipole coupling. The process is thus described as a virtual electromagnetic transition followed by a real collision. Now consider the reverse process where energy is stored in the upper p level of the second atom, and radiation at the same frequency ω is again present. As the atoms approach each other they each make virtual transitions in the opposite direction to the arrows denoted by (2). The process is completed by the emission of a photon of frequency ω. The overall process is thus described as a virtual collision followed by a real emission. For collision velocities high enough that a straight-line trajectory is a good approximation, the collision cross sections for the forward and reverse processes are equal.

We next consider the process from the viewpoint of an electromagnetic transition between the states of the quasi-molecule which is formed during the time of a collision between an A and B atom. Fig. 3 shows the energy of the quasi-molecular state as a function of the distance between

VIRTUAL TRANSITION VIEWPOINT

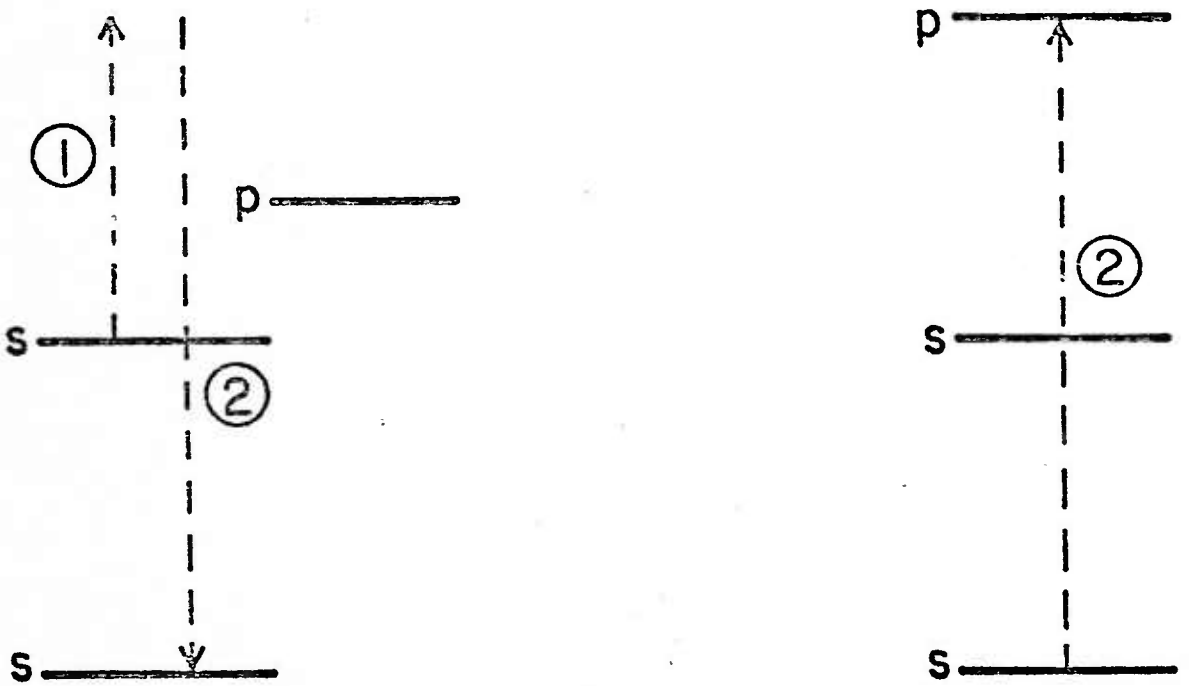

Fig. 2--Virtual transition viewpoint of laser induced collisions. For flow of energy from the left- to the right-hand atom, the process is best considered as a virtual electromagnetic transition followed by a real collision. For the reverse process, we view the process as a virtual collision followed by a real transition.

the colliding atoms. The lower state represents the sum energy of an excited A atom and a ground state B atom, while the upper state is the final state, where B is excited and A is at ground. This viewpoint leaves out the dynamics of the intermediate state and is thus not always correct. In any case it is somewhat misleading. Using stationary perturbation theory one calculates a matrix element between the initial and final states of the quasi-molecule. Since the square of this matrix element varies as $1/R^6$, one might at first expect the electromagnetic absorption to increase in strength as the atoms approach each other, and thus expect a broad linewidth (at least several hundred wavenumbers) as a function of the energy of the incident photon $\hbar\omega$. More exact analysis shows that the square of the effective interaction time between the colliding species varies inversely as the slope of the relative energy difference of the initial and final states and thus increases as R^7. An additional R^2 dependence is introduced when integrating over impact parameter. We will see that the linewidth for the dipole-dipole process is in fact quite narrow and peaks at the $R = \infty$ energy separation of the colliding atoms.

Following the reasoning of Fig. 3, one expects the collision cross section to peak at the $R = \infty$ energy separation for dipole-dipole and dipole-quadrupole processes. For quadrupole-quadrupole, spin exchange, charge exchange, and free-bound processes a peak at the $R = \infty$ frequency is not expected.

The third viewpoint is ad hoc. In this viewpoint the electromagnetic field applied to atom A causes an effective per atom dipole moment at the sum frequency of the energy stored in atom A and the applied field. Each A atom possesses a near electric field often many orders of magnitude larger than the macroscopic electric field. As an A atom passes a B atom an electromagnetic transition of the B atom is induced. The dephasing event allowing the transition is simply the passage of the A atom by the B atom; and the expected linewidth of the process is roughly the reciprocal of the transit time, or about 1 cm^{-1} at thermal velocities.

I now give a brief description of the theory. The overall procedure is to apply perturbation theory at fixed interatomic separation R ; to integrate over R(t) for fixed impact parameter ρ and velocity $\bar{V}$; and to then integrate over ρ and $\bar{V}$. The principal assumptions are that the collisions are slow compared to the orbiting velocity of an electron, and

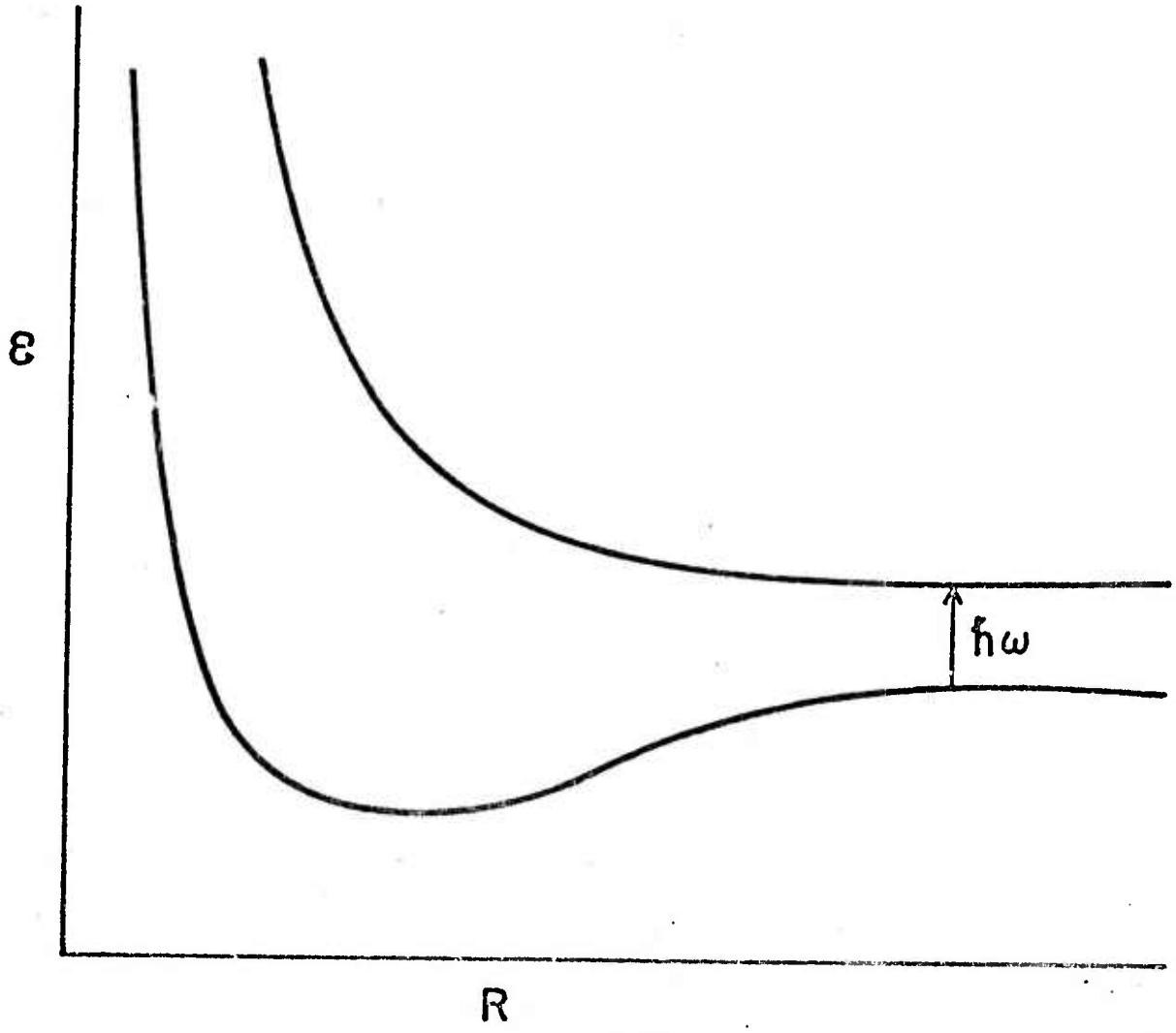

$$|\langle 1|x|2\rangle|^2 \sim 1/R^6$$

$$|\Delta t|^2 \sim \left[\frac{1}{\bar{V}} \; \frac{1}{\hbar} \; \frac{1}{\partial\mathcal{E}/\partial R}\right] \sim R^7$$

Fig. 3--Quasi-molecular viewpoint of laser induced collisions. A photon of frequency ω causes an electromagnetic transition between the initial and final state of the quasi-molecule.

that the net energy defect is small compared to the incident energy of the particles, thus implying that the trajectories are unchanged. We work in a basis set of product eigenfunctions of the separated atoms. Thus

$$\psi = \sum_n c_n(t)\, u_n \exp - jE_n t/\hbar \tag{1}$$

The u_n are the product eigenfunctions of the atomic states and the E_n are the sum energies.

The classical interaction hamiltonian is

$$H' = ex_1E + ex_2E + \frac{e^2 x_1 x_2}{R^3} \tag{2}$$

where x_1 and x_2 are the local coordinates of the electrons of each atom, E is the applied electromagnetic field, and R is the distance between atoms. The first two terms represent the interaction of the electromagnetic field with each atom separately while the latter term gives the dipole-dipole coupling between the two atoms. Following the notation of Fig. 1 we assume three pertinent product states. c_1 is the amplitude of the product state whose energy is the sum of the storage s state of the first atom and the ground state of the second atom. c_2 is the amplitude of the p state of atom A and the ground state of atom B, while c_3 is the amplitude of the upper p state of atom B and the ground state of atom A. We consider the on line center case where $\hbar\omega_D$ = the energy defect ΔE. Substituting into Schrödinger's equation we obtain

$$\frac{\partial c_1}{\partial t} = \frac{1}{j\hbar} \frac{\mu^{A1} E}{2} c_2 \exp j\Delta\omega_D t \tag{3a}$$

$$\frac{\partial c_2}{\partial t} = \frac{1}{j\hbar} \frac{\mu^{A1} E}{2} c_1 \exp - j\Delta\omega_D t + \frac{1}{j\hbar} \frac{\mu^{A2}\mu^{B}}{R^3(t)} c_3 \exp - j\Delta\omega_D t \tag{3b}$$

$$\frac{\partial c_3}{\partial t} = \frac{1}{j\hbar} \frac{\mu^{A2}\mu^{B}}{R^3(t)} c_2 \exp j\Delta\omega_D t \tag{3c}$$

$\Delta\omega$ is the energy separation of the upper p levels, as shown in Fig. 1. μ^{A1}, μ^{A2}, and μ^{B} are defined as: $\mu^{A1} = \langle 1|x_1|2\rangle^{A}$, $\mu^{A2} = \langle 2|x_1|0\rangle^{A}$, and $\mu^{B} = \langle 1|x_2|0\rangle^{B}$.

If the relative rate of change of c_1, c_3, and $1/R^3(t)$ are slow compared to $\Delta\omega$ then (3b) may be integrated and combined into (3a) and (3c) to yield coupled equations between the initial and final states. These two coupled states have an effective interaction hamiltonian

$$H_{13} = H_{31} = \left(\frac{\mu^{A1}E}{2\hbar\Delta\omega}\right) \frac{\mu^{A2}\mu^{B}}{R^3(t)}$$

By varying the strength of the electromagnetic field E, the strength of the interaction hamiltonian may be varied. By varying the frequency of the electromagnetic field an effective curve crossing may be created at arbitrary R.

By a change of variable of the form

$$c_i = a_i \exp\left[-\frac{j}{\hbar}\int_{-\infty}^{t}\frac{C_6}{R^6(t)}\,dt\right]$$

(3) become

$$\frac{\partial a_1}{\partial t} = \frac{H_{13}}{j\hbar}\, a_3 \exp\left[-\frac{j}{\hbar}\int_{-\infty}^{t}\frac{C_6}{R^6(t)}\,dt\right] \tag{4a}$$

$$\frac{\partial a_3}{\partial t} = \frac{H_{13}}{j\hbar}\, a_1 \exp\left[\frac{j}{\hbar}\int_{-\infty}^{t}\frac{C_6}{R^6(t)}\,dt\right] \tag{4b}$$

In these equations I have neglected a small ac Stark shift which for the power densities which we will consider will be (at most) a few tenths of a cm^{-1}. The (relative) van der Waals constant C_6 includes not only terms which come directly from (3), but also all other contributions pertinent to the difference of the energy shifts between the initial and final states. This shift is quite important and sets the minimum impact parameter which contributes to the interaction.

We now examine the weak-field case where for all impact parameters we may neglect the depletion of a_1. We take $R(t) = [\rho^2 + \bar{v}^2t^2]^{\frac{1}{2}}$.

We assume a constant impact parameter ρ and integrate (4b) over $t = -\infty$ to $t = +\infty$. For impact parameters such that the exponent in

(4b) is less than about 1 radian, the transition probability as a function of impact parameter is

$$|a(\rho)|^2 = \frac{1}{\hbar^4}\left(\frac{\mu^{A1}\mu^{A2}\mu^{B}}{\Delta\omega\bar{V}\rho^2}\right)^2 \tag{5}$$

The cross section for collision is now obtained by integrating over all impact parameters from ρ_0 to infinity, or

$$\sigma_c = 2\pi\int_{\rho_0}^{\infty}|a(\rho)|^2\,\rho d\rho$$

Combining the above we obtain the result

$$\sigma_c = \frac{\pi}{\hbar^4}\left(\frac{\mu^{A1}\mu^{A2}\mu^{B_E}}{\bar{V}\Delta\omega\rho_0}\right)^2 \tag{6a}$$

where

$$\frac{1}{\hbar}\int_{-\infty}^{+\infty}\frac{C_6}{R^6(t)}\,dt \cong \frac{3\pi}{8}\frac{|\mu^{A2}|^2|\mu^{B}|^2}{\hbar^2\bar{V}\Delta\omega\rho_0^5} = 1 \tag{6b}$$

The second part of (6b) determines the minimum impact parameter ρ_0 which is to be used in (6a).

If we assume that all involved transitions have relatively large oscillator strength, then at thermal velocities, ρ_0 will typically be greater than 10 Å and the details of the atomic potentials for small interaction distances need not be considered. For $\Delta\omega \cong 5000\ cm^{-1}$, typical predicted collision cross sections are about $\sigma_c \cong 5\times10^{-23}\frac{P}{A}\ (W/cm^2)\ cm^2$. Thus an incident power density of about 1 MW/cm^2 is required to obtain cross sections of atomic dimension. Though I will not go into detail here, it is expected that the cross section for collision will continue to increase linearly with power density until reaching approximately $\pi\rho_0^2$. We believe that collision cross sections as large as $10^{-13}\ cm^2$ should be obtainable, and experiments to demonstrate such cross sections are underway.

To this point we have considered the cross section for collision induced by a laser tuned to the $R = \infty$ frequency of the separated atoms. The expected line shape as a function of the frequency of the transfer laser is of considerable interest. If it were not for the dependence of the eigenenergies of the quasi-molecular states on the interatomic spacing then the line shape for transfer would be a first order modified Bessel

function of the third kind with argument $(2\pi\Delta f\rho_0/\overline{V})$, where Δf is the frequency defect. For a situation such as that in Fig. 3 where the energy level of the lower quasi-molecular state falls faster than the upper state, a quite rapid fall-off is expected on the low frequency side of the $R = \infty$ frequency. On the high frequency side, the tunable laser in effect causes a curve crossing at arbitrary R . One might intuitively expect a sharp fall off on the red side, and a slowly varying tail on the blue side. Further work — both theoretical and experimental — is necessary.

Experimental Results

In a recent experiment, we attempted to demonstrate a laser induced collision in a mixture of Sr and Ca [6]. The system studied is shown in Fig. 4. The collision process is described by

$$Sr(5p\,^1P^0) + Ca(4s^2\,^1S) + \hbar\omega(6409\ \text{Å}) = Sr(5s^2\,^1S) + Ca(4d\,^1D) \qquad (7)$$

Energy was first stored in the radiatively trapped $5p\,^1P^0$ level of Sr I. This level was populated by two-photon pumping of the $5d\,^1D$ Sr level, followed by radiative decay. Inelastic collision to the $4d\,^1D$ level of Ca I should be produced by a second laser beam at 6409 Å.

During collision of an excited $Sr(5p\,^1P^0)$ and a ground state $Ca(4s^2\,^1S)$ atom the strong dipole-dipole coupling of the (5p-5s) Sr transition and the (4p-4s) Ca transition causes a virtual transition of a Ca atom. Absorption of the 6409 Å photon completes the Ca excitation. The process is thus viewed as a virtual collisional excitation, followed by a real absorption. For this experiment, $\hbar\Delta\omega = 1954\ \text{cm}^{-1}$, and (6) predicts $\rho_0 = 16.7$ Å , and $\sigma_c = 2.9 \times 10^{-23}\ \frac{P}{A}\ (\text{W/cm}^2)\ \text{cm}^2$.

We now believe that the previously reported experiment [6] can no longer be considered a demonstration of these effects. The difficulty arises due to the presence of a transition at 6408.5 Å within the triplet series of Sr (see Fig. 4). This transition differs by only .1 Å from the interatomic frequency of 6408.6 Å, and is beneath our resolution. A possible (and likely) artifact path now consists of collisional transfer from the Sr 5p to Sr $4d\,^3D$ levels, followed by laser excitation at 6408.5 Å and collisional transfer to the Ca $4d\,^1D$ level. The reported linearity with 6409 Å power density up to about 10^7 W/cm^2 might be explained by a process of (saturated) selective laser excitation, followed by ionization and charge exchange with Ca.

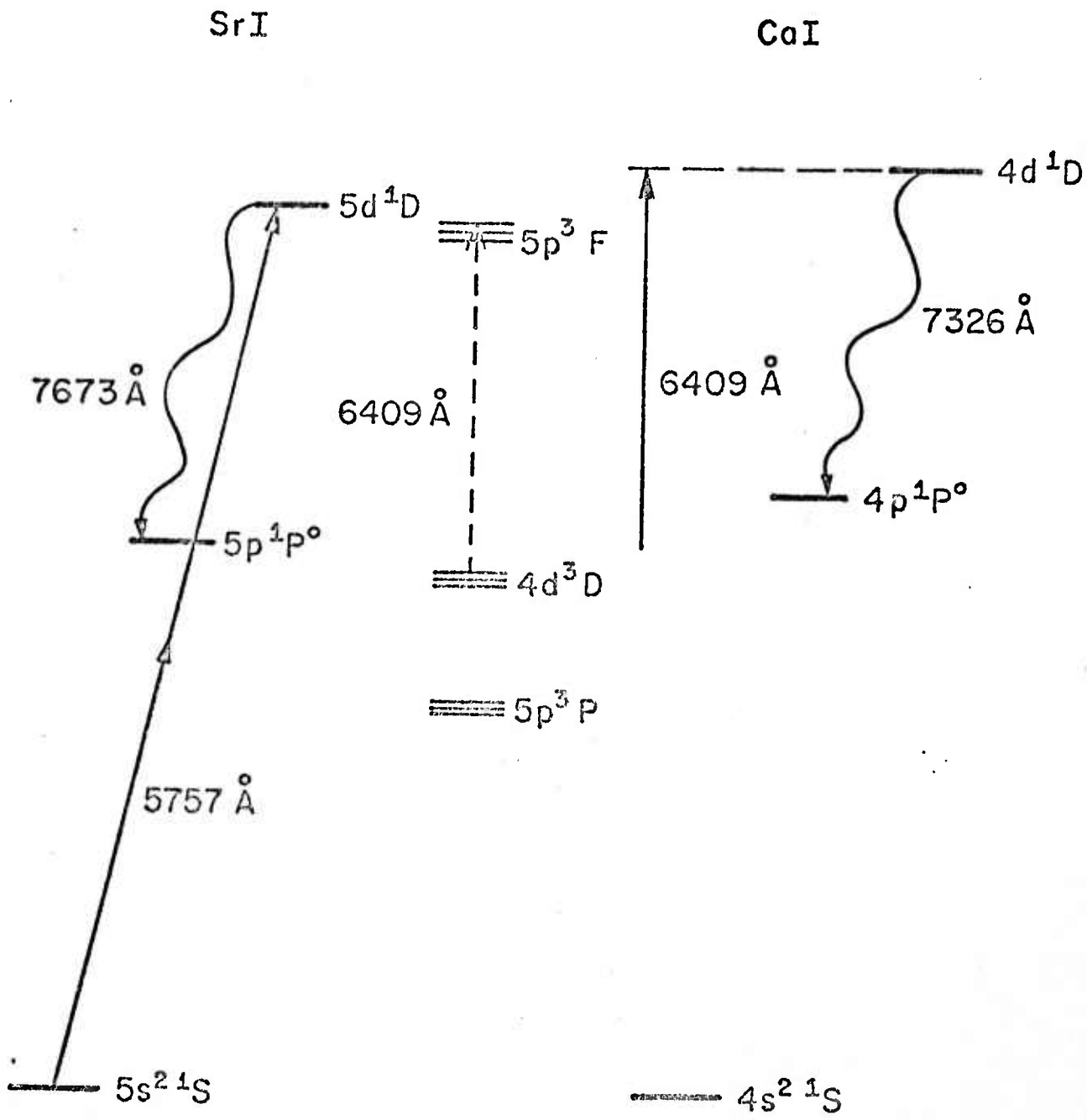

Fig. 4--Energy level diagram for Sr-Ca induced-collision experiment.

Our tentative conclusion that the experiment is no longer valid is based primarily on the observation of Ca 7326 Å fluorescence of comparable magnitude when the transfer laser is tuned to 6409 Å or to other lines in the same triplet series.

Further experimental work on the Sr-Ca system and on other related systems is now underway.

Applications

I will now briefly describe a number of potential applications and devices which may result from collisional processes of this type. We first consider a radiative collision laser [1]. A schematic of a radiative collision laser is shown in Fig. 5. In a laser of this type energy would be stored in the radiatively trapped resonance line of Sr. During collision with a Tℓ atom, a Sr atom would be de-excited while a Tℓ would be excited from ground to the Tℓ $6p^2P^0$ $[1\frac{1}{2}]$ level. A photon at 7190 Å would experience gain rather than loss. The gain coefficient g is related to the collision cross section σ_c according to

$$g = \frac{N_A N_B \bar{V} \omega \sigma_c}{P/A} \qquad (8)$$

where N_A and N_B are the number density of the two species. If we take $\sigma_c = 10^{-22}$ P/A , $N_A = 10^{16}$ atoms/cm^3 , $N_B = 10^{19}$ atoms/cm^3 , $\omega = 10^5$ radians/sec , and $\bar{V} = 10^5$ cm/sec , we find a gain cross section of $g = 0.1$ cm^{-1} . This number is somewhat optimistic for a typical system. A laser of this type may be of practical interest for two reasons: First, is the attractive possibility of radiatively trapped resonance line storage. Second, is the variable gain cross section provided by varying the number density of the second (ground state) species.

Though most of the discussion of this paper has been concerned with a single-photon transfer process, all ideas continue to hold for a multi-photon process. By storing energy in high lying states of atoms or ions, and then using multi-photon processes with the intense VUV light sources now available, it should be possible to reach states to at least the 100 Å spectral region.

Coherent collisionally induced Raman processes such as that shown in Fig. 6 may be of interest for up-conversion of long wavelength radiation.

RADIATIVE COLLISION LASER

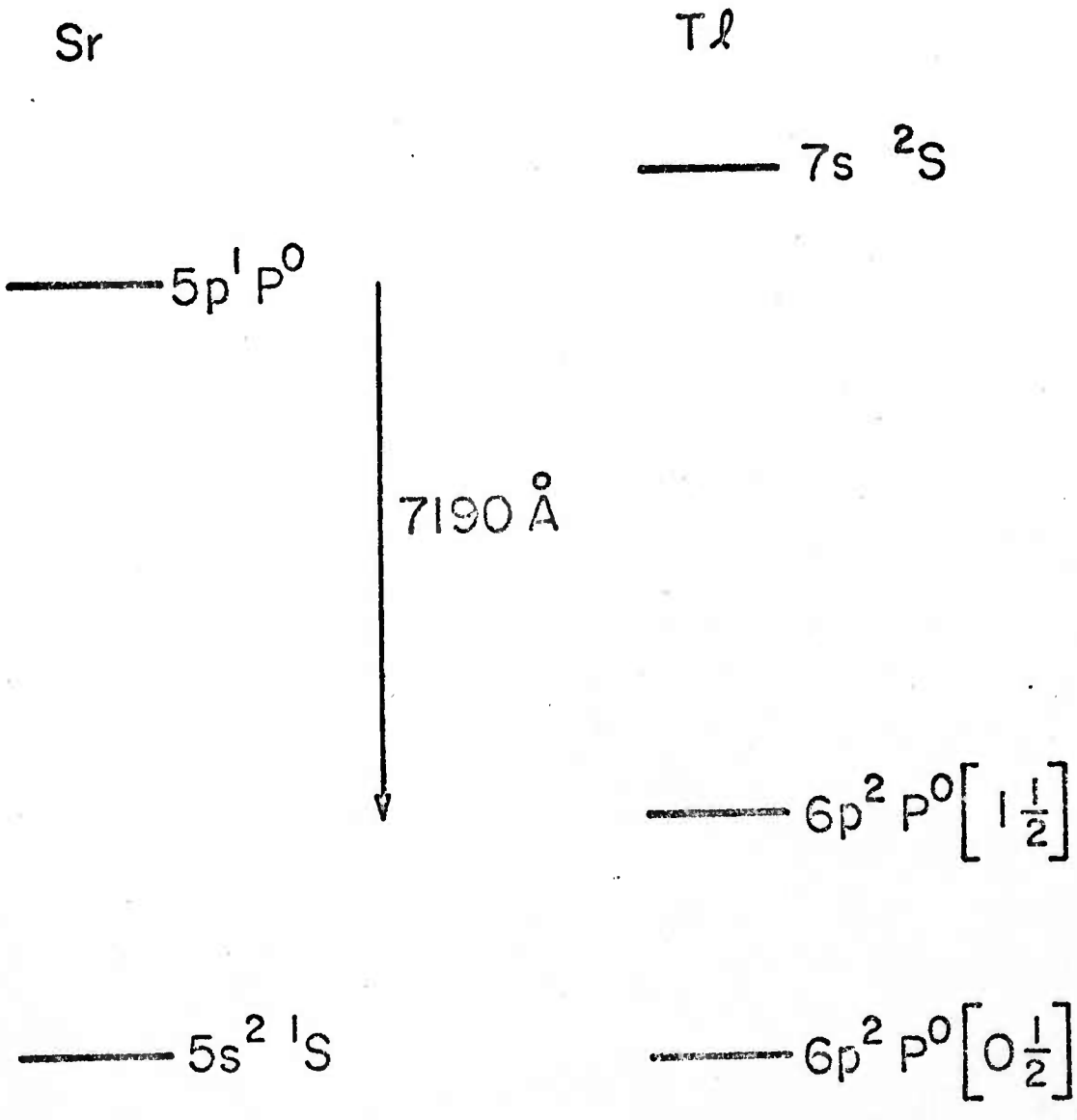

Fig. 5--Energy level diagram of a possible radiative collision laser.

COHERENT RAMAN PROCESSES

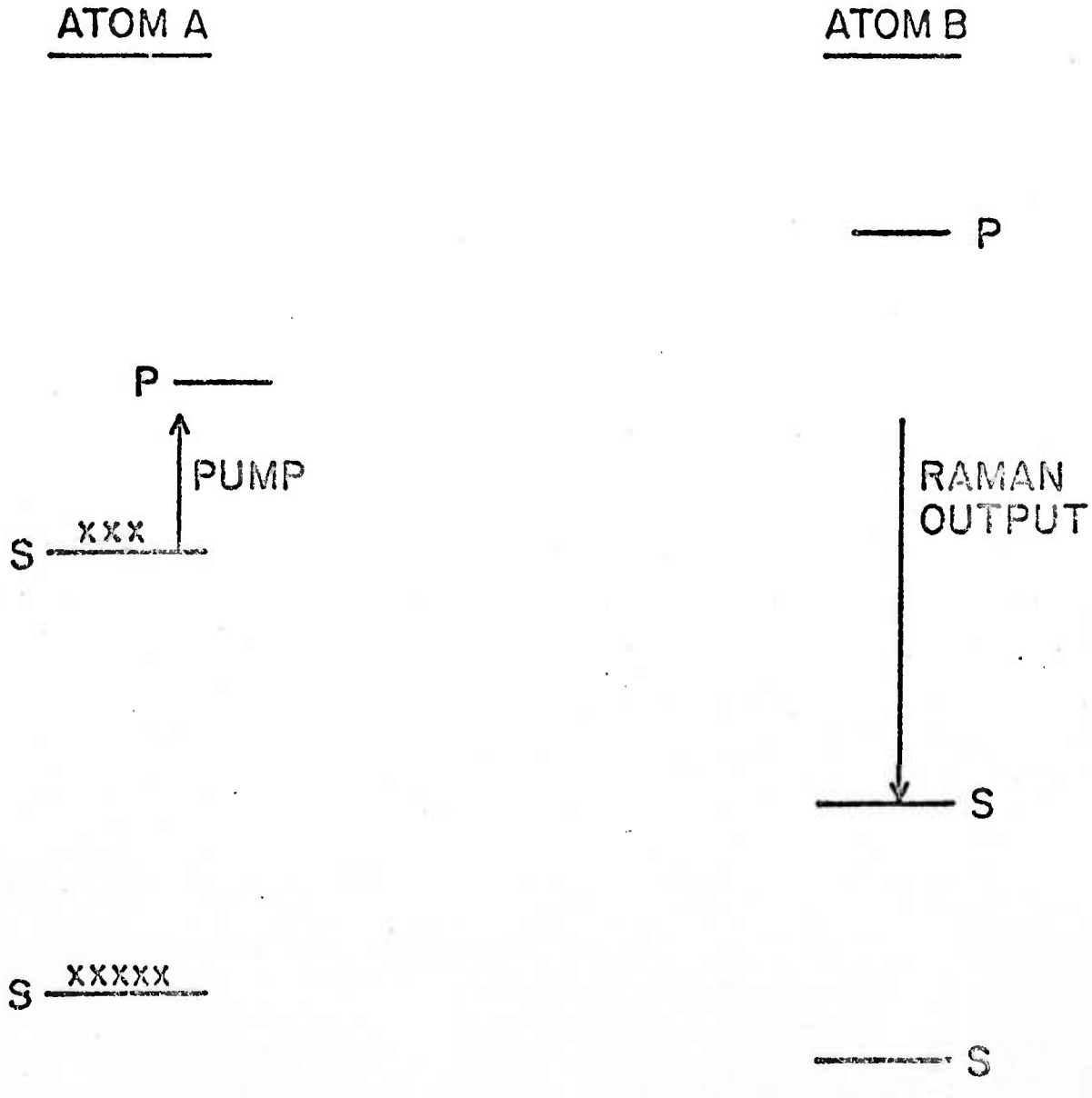

Fig. 6--In a coherent collisional Raman process gain is obtained at the Raman output frequency. Note that atom A need not be inverted, and that the frequency of the Raman output may be higher than that of the pumping frequency.

This process is alternately described as a collisionally aided Stokes process which allows an output frequency higher than the input frequency, or alternately as an anti-Stokes process in a quasi-molecular system. The ability to demonstrate processes of this type will be dependent on achieving high number densities of the ground state species.

Other areas of application of these processes include the selective ionization of innershell electrons, laser induced charge transfer collisions, and perhaps radiative charge transfer lasers.

Laser induced collisions may someday allow one to direct the flow of energy and thus to influence reaction rates of general gas phase kinetic processes.

The authors acknowledge many helpful discussions with Dr. David Bloom, Mr. William Green, and Mr. Jonathan White. We wish to thank Mr. Ben Yoshizumi for help with the experiments reported here.

List of References

* This work was jointly supported by the U.S. Office of Naval Research, the Advanced Research Projects Agency, and the Energy Research and Development Administration.

1. L. I. Gudzenko and S. I. Yakovlenko, Zh. Eksp. Teor. Fiz. 62, 1686 (1972) [Sov. Phys. JETP 35, 877 (1972)].
2. S. E. Harris and D. B. Lidow, Phys. Rev. Lett. 33, 674 (1974), and 34, 172(E) (1975).
3. M. G. Payne and M. H. Nayfeh, "Laser Enhanced Collisional Energy Transfer" (to be published).
4. Sydney Geltman, "Theory of Laser-Stimulated Collisional Excitation Transfer" (to be published).
5. Thomas F. George, Jian-Min Yuan, I. Harold Zimmerman, and John R. Laing, "Radiative Transitions for Molecular Collisions in an Intense Laser Field," Disc. Faraday Soc. No. 62.
6. D. B. Lidow, R. W. Falcone, J. F. Young, and S. E. Harris, Phys. Rev. Lett. 36, 462 (March 1976).

List of Figures

1. Schematic of laser induced collision process. Energy is stored in the s state of atom A and may be rapidly transferred to the upper p state of atom B .
2. Virtual transition viewpoint of laser induced collisions. For flow of energy from the left- to the right-hand atom, the process is best considered as a virtual electromagnetic transition followed by a real collision. For the reverse process, we view the process as a virtual collision followed by a real transition.
3. Quasi-molecular viewpoint of laser induced collisions. A photon of frequency ν_0 causes an electromagnetic transition between the initial and final state of the quasi-molecule.
4. Energy level diagram for Sr-Ca induced-collision experiment.
5. Energy level diagram of a possible radiative collision laser.
6. In a coherent collisional Raman process gain is obtained at the Raman output frequency. Note that atom A need not be inverted, and that the frequency of the Raman output may be higher than that of the pumping frequency.